

Influence of Coadsorbates on the NO Dissociation on a Rhodium(311) Surface

Oliver R. Inderwildi,^{*[a]} Dirk Lebiedz,^[a] Olaf Deutschmann,^[b] and Jürgen Warnatz^[a]

Density functional theory (DFT) studies were performed to investigate the influence of coadsorbates on the nitrogen oxide dissociation on the vicinal rhodium(311) surface. This study amplifies prior studies on the dissociation of oxygen and nitrogen oxide on the (111) facet of rhodium. The influence of coadsorbates on the kinetic parameters and thermochemistry of the NO dissociation

on Rh(311) was studied. In addition, the activation energy and thermochemistry of this reaction were determined as a function of oxygen preoccupation/initial coverage. Steric and electronic effects and their influence on the dissociation reaction were examined. The results are discussed in the face of an NO_x dissociation catalyst system proposed by Nakatsuji.

Introduction

The increase of the green-house-gas concentration in the Earth's atmosphere and the associated climate change is believed to be the most severe threat we are facing.^[1] Therefore, legislations in industrial countries are aiming towards the reduction of the green-house-gas emissions. The main green-house gas is carbon dioxide and its main source is combustion, mainly in automotive engines. A possibility to reduce the emission of CO₂ is to operate gasoline engines under oxygen-rich (fuel-lean) conditions, because under these conditions combustion engines are more fuel-efficient. The major drawback of lean-run car engines is the increased emission of nitrogen oxides (NO_x, x=1,2) and soot. To overcome these drawbacks, the removal of NO_x^[2] and soot^[3] is a widespread topic in academic and industrial research. An exhaust-gas aftertreatment system that reduces NO_x was suggested by Nakatsuji.^[4] A rhodium-based catalytic converter, periodically operated under alternating fuel-lean and fuel-rich conditions, efficiently removes NO_x from the automotive exhaust and is sulphur-resistant. However, the surface chemistry of this system is not fully understood.^[5,6]

A previous density functional theory (DFT) study of the NO dissociation on Rh(111) indicates that the perfectly planar (111) facet is rather inactive towards NO dissociation with or without oxygen preoccupation (high activation barrier and endothermic process). However, it is known that stepped surfaces are by far more active. DeLouise et al.^[7] observed, for example, that Rh(331) is an order of magnitude more active than Rh(111) in the NO dissociation. The step-enhanced activity of metal catalysts has been experimentally^[8–10] as well as theoretically^[11] investigated in recent years.

The higher activity of step sites is also the reason why a growing nanosized metal particle on supportive oxides is an important topic in heterogeneous catalysis. The small metal particles contain a significant amount of surface defects and are therefore more active. Against this background, the dissoci-

ation of NO on the stepped (311) facet of rhodium was investigated by density functional theory (DFT).

The vicinal (311) surface of rhodium has not been studied as thoroughly as its low-index counterparts. Numerous publications are concerned with helium scattering on clean Rh(311)^[12] and hydrogen scattering on Rh(311).^[13] Payne et al.^[8] studied a Rh(311) surface with hydrogen adsorbed by low electron energy diffraction (LEED) and thermal desorption spectroscopy (TDS). However, studies on the interaction of NO with the (311) facet of rhodium are rare. A fast X-ray photoelectron spectroscopy (XPS) study by Esch et al.^[14] addresses the uptake of NO on different stepped rhodium surfaces. Janssen et al.^[9] studied the interaction of NO with different stepped surfaces by TDS. DFT investigations of Rh(311) by Sun et al.^[15] as well as LEED studies by Liepold et al.^[16] cover the multilayer relaxation of Rh(311). Herein, in particular the influence of preoccupation on the NO dissociation reaction is investigated by density functional calculations.

Ab initio DFT calculations are becoming a useful tool to estimate kinetic parameters of detailed surface reaction mechanisms for reasons explained in a foregoing publication.^[6] Particularly the determination of the surface coverage dependencies of surface reactions by DFT methods^[17] is of general interest, because this information is not easily accessible by conventional experimental techniques. Models based on detailed elemen-

[a] Dr. O. R. Inderwildi, Dr. D. Lebiedz, Prof. Dr. J. Warnatz
Interdisciplinary Centre for Scientific Computing of the
University of Heidelberg, Im Neuenheimer Feld 368
69120 Heidelberg (Germany)
Fax: (+49) 6221-54-8884
E-mail: oliver.inderwildi@iwr.uni-heidelberg.de

[b] Prof. Dr. O. Deutschmann
Institute of Chemical Technology and Polymer Chemistry
University of Karlsruhe, Engesserstr. 20
76131 Karlsruhe (Germany)

tary-step reaction mechanisms are becoming more popular than those based on global mechanisms, owing to their higher accuracy and the permanent acceleration of computer processor speed.^[18]

Computational Details

Herein, the reactions of nitrogen monoxide on Rh(311) have been studied by means of DFT calculations using CASTEP (Cambridge Sequential Total Energy Package).^[19] The generalised gradient approximation (GGA) as proposed by Perdew et al.^[20] was applied, combined with Vanderbilt ultrasoft pseudopotentials.^[21] The plane-wave basis set was truncated at a kinetic energy of 300 eV. The reciprocal space of the (2×2) and (1×1) unit cells were sampled with a (2×4×1) and (4×8×1) k-point mesh, respectively, as generated by the Monkhorst–Pack scheme.^[22] In density-of-state calculations, the Brillouin zone was sampled with a denser k-point mesh, that is, (2×5×2) and (6×10×2) for the (2×2) and (1×1) unit cell, respectively.

The surface was modelled by a preoptimised rhodium slab with a thickness of six atomic layers. For the preoptimisation procedure see the first paragraph of the Results and Discussion section. Periodic boundary conditions are extrapolated from a metal cluster to an extended surface. A 10-Å vacuum region was placed in between the periodic slabs to ensure that the adsorbate and the subsequent slab do not interact.

To determine the adsorption energies ΔE_{ads} , the target surface was geometry-optimised with and without the adsorbate; the energies of the optimised surfaces were subsequently calculated. The geometry of the adsorbate was optimised within a supercell, identical to the cell of the surface, and the energy of this optimised adsorbate ($E_{\text{adsorbate}}$) was subsequently calculated. Finally, the adsorption energies were determined according to Equation (1):

$$\Delta E_{\text{ads}} = E_{\text{slab+adsorbate}} - (E_{\text{slab}} + E_{\text{adsorbate}}) \quad (1)$$

To determine the thermochemistry ($\Delta E_{\text{reaction}}$) and the activation barrier (E_a) of a surface reaction, structures of the reactants and products were optimised. Subsequently, the transition state of the surface transformation was located on the potential energy hypersurface (PES) by performing a linear synchronous calculation, combined with a quadratic synchronous transit calculation and conjugate gradient refinements.^[23] The total energies of the reactants, the transition state and the products were computed. The reaction energies ($\Delta E_{\text{reaction}}$) were calculated according to Equation (2):

$$\Delta E_{\text{reaction}} = E_{\text{products}} - E_{\text{reactants}} \quad (2)$$

in which E_{products} stands for the single-point energy of the product structure and $E_{\text{reactants}}$ for the single-point energy of the reactant structure. The activation energy (E_a) was calculated according to Equation (3):

$$E_a = E_{\text{transition state}} - E_{\text{reactants}} \quad (3)$$

in which $E_{\text{transition state}}$ denotes the single-point energy of the transition-state structure.

The electron transfer was investigated by Mulliken population analysis. Mulliken population analysis was carried out using the formalism described by Segall et al.^[24] While charges, calculated by Mulliken population analysis, are a means to monitor relative electron transfer, they do not reflect accurate, absolute charges.

The metal d-states were investigated by calculating the d-state-projected density of states (d-PDOS). The difference in the d-state population was calculated by subtracting the d-state population of clean rhodium ($n_{\text{d,Rh}}$) from rhodium with adsorbates ($n_{\text{d,Rh+Ad}}$) according to Equation (4):

$$\Delta n_{\text{d}}(\varepsilon) = n_{\text{d,Rh+Ad}}(\varepsilon) - n_{\text{d,Rh}}(\varepsilon) \quad (4)$$

The d-state population difference can then be calculated according to Equation (5):

$$\Delta n_{\text{d}} = \int_{-\infty}^{\varepsilon_{\text{F}}} \Delta n_{\text{d}}(\varepsilon) \text{d}\varepsilon \quad (5)$$

The energy change of the d-electrons upon adsorption was calculated according to Equation (6):

$$\Delta E_{\text{d}} = \int_{-\infty}^{\varepsilon_{\text{F}}} \Delta n_{\text{d}}(\varepsilon) \varepsilon \text{d}\varepsilon \quad (6)$$

Results and Discussion

Rhodium(311) Plane—Preoptimisation of the Surface

Prior to the investigation of surface processes on Rh(311), the surface of the rhodium slab was optimised in order to ensure that it is not in a chemically activated state.

The geometry of a (1×1) unit cell of a ten-layer slab Rh(311) with the four upper mobile layers (Figure 1, light grey atoms) and six residual rhodium layers (dark grey atoms), constrained at their positions in the bulk structure, was optimised. A 10-Å vacuum region was placed between the periodic slabs to ensure that the adsorbate and the subsequent slab are not interacting.

In analogy to LEED^[16] and previous DFT^[15] studies of multi-layer relaxation of Rh(311), the interlayer spacing of the top layers behaves oscillatory and the relaxation decreases from the top to the lower layers of the surface.

The interlayer spacing between the two top layers $d_{1,2}$ and between the third and fourth layer $d_{3,4}$, decreases, while it increases between the second and third layer $d_{2,3}$ and between the fourth and fifth layer $d_{4,5}$. The calculated values of the interlayer relaxations (Δd [%]) of the optimised slab resemble the values found by LEED analysis within the experimental error limits (see Table 1).

To keep the calculation time for the PES of the surface transformations short, the slab thickness was decreased for investigations of surface processes. The lower four layers of the pre-optimised slab were removed and the upper four layers were constrained at their position on the optimised surface. Furthermore, the (1×1) unit cell was expanded to a (2×2) unit cell so that surface coverage can be modified over a broad range (see Figure 1). The surface coverages were varied in analogy to a previous DFT study on Rh(111).^[5,6]

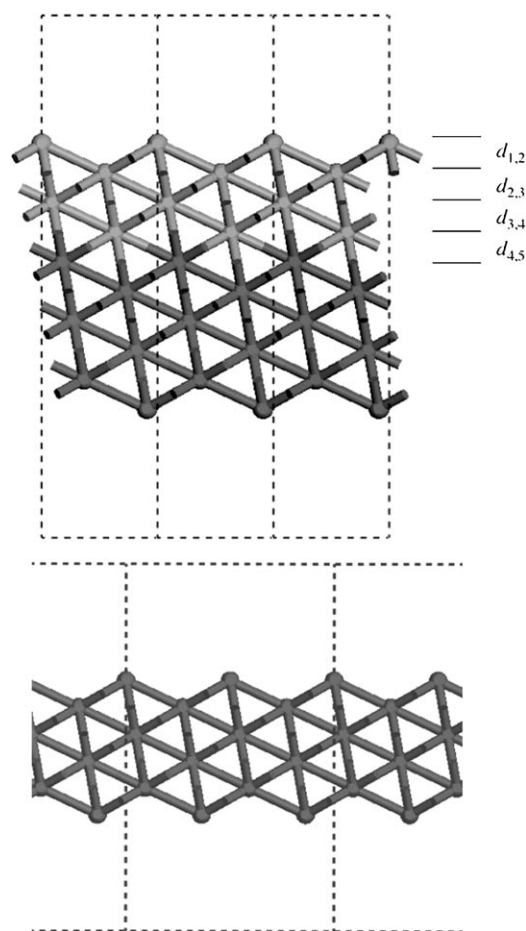


Figure 1. Ten-layer (1×1) (top) and six-layer (2×2) (bottom) unit cell of Rh(311).

Table 1. Comparison of the multilayer relaxation of Rh(311).			
	DFT	DFT ^[a]	LEED
$\Delta d_{1,2}$ [%]	-14.9	-16.2	-14.5 ± 1.8
$\Delta d_{2,3}$ [%]	+6.8	+6.2	$+4.9 \pm 2.0$
$\Delta d_{3,4}$ [%]	-1.7	-2.6	-1.9 ± 2.0
$\Delta d_{4,5}$ [%]	+0.9	0	-
$d_{1,2}$ [Å]	0.98		
$d_{2,3}$ [Å]	1.22		
$d_{3,4}$ [Å]	1.13		
$d_{4,5}$ [Å]	1.16		

[a] Results of an earlier DFT study, taken from ref. [15].

NO Adsorption on Rh(311)

Prior to the investigation of the NO dissociation reaction, the different possible adsorption sites of NO, atomic nitrogen and atomic oxygen on Rh(311) and the corresponding adsorption energies were determined.

In Figure 2 a Rh(311) surface with labels for the possible adsorption sites is shown. Adsorption energies are given in Table 2.

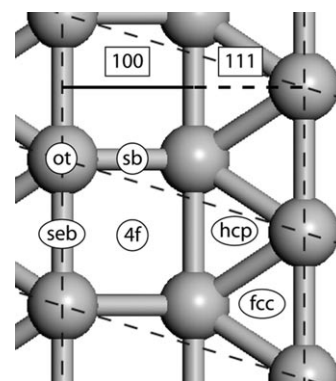


Figure 2. Possible adsorption sites on Rh(311).

Table 2. Adsorption energies of NO, N and O on different sites of (1×1)-Rh(311).^[a]

Adsorption Site	NO	O	N
step-edge on top	-2.72	-1.65	1.17
step-edge bridge	-1.42	-2.45	0.49
step bridge	-2.75	-2.26	0.43
step fourfold hollow	-2.43	unstable	0.21
terrace threefold hollow			
fcc	-2.49	-2.17	0.09
hcp	-3.05	-2.58	-0.28

[a] Adsorption energies are referenced to stable molecules in the gas phase. Therefore, the adsorption energies of atomic adsorbates (N, O) are relative to their saturated parent molecule, namely, N₂ and O₂, respectively.

Atomic oxygen binds strongest to the hcp site of the (111) terrace, but also to bridged (twofold) sites on the (100) step (step bridge, step-edge bridge). Atomic nitrogen also binds strongest to the hcp site of the (111) terrace. NO seems to bind strongest to the hcp threefold site of the (111) terrace with the oxygen leaning towards the step site. According to these calculations this threefold position is energetically favoured over the on-top position (see Table 2). However, it is known that GGA functionals such as the used PW91 functional yield too small 5σ-to-2π* gaps (HOMO–LUMO separation) and therefore the backdonation is enhanced. In high coordination sites the bonding is dominated by the interaction with the 2π* orbital of π-acceptor adsorbates, while the bonding is dominated by the interaction with the 5σ orbital in the case of on-top sites. Therefore, high coordination sites are favoured over low coordination sites according to GGA calculations, which is in clear contrast to experimental observations.^[25] Since experimental studies of nitrogen oxides on Rh(311) are not available so far, it cannot be excluded that the calculated structure is indeed the most stable or an artefact of this overbinding effect. However, in the case of corrugated Ru, the DFT study by Hammer^[26] shows that NO resides with the N atom on the

base of a step and the O atom leaning towards the edge of the step in analogy to our findings.

Even though the on-top NO species on the step edge might be more stable, the dissociation is less likely to occur on those sites. This assumption is supported by the calculations of the NO dissociation on corrugated Ru surfaces, where the dissociation barrier for species parallelly adsorbed to steps is found to be lowest.^[26] Thus, for the calculation of the NO decomposition, the hcp threefold site was chosen as a starting point.

NO Dissociation on Rh(311)

As mentioned above, NO was calculated to be most stable when coordinated in a threefold position perpendicular to the (111) terrace, with the oxygen atom leaning towards the step edge (see Figure 3, left).

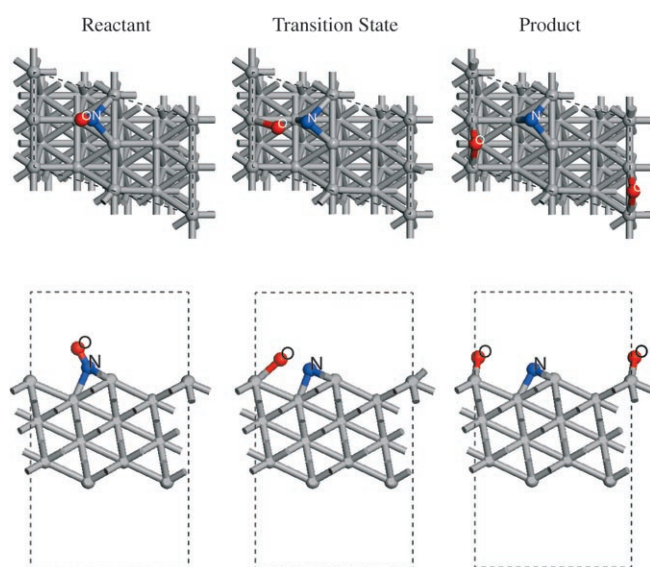


Figure 3. Nitrogen monoxide dissociation on Rh(311).

The most likely adsorption geometry of atomic oxygen after dissociation was determined to be in the step-bridged position of the (100) plane (see Figure 3), while atomic nitrogen remains in the threefold position of the (111) terrace (it is known that the atomic oxygen on Rh(100) is most strongly bound in the bridged position^[27]). These results are again in analogy to the findings for NO dissociation on a corrugated Ru(0001) surface.^[26] The nitrogen in the product structure is slightly closer to the (111) plane, indicating that it is bound stronger to the surface.

Calculating the PES for the dissociation supports this assumption. The reaction was calculated to be exothermic with a reaction energy of -0.52 eV.

The transition state is located at 0.49 of the reaction coordinate, where zero denotes the reactant and 1 the product geometry. The oxygen is bound to the closer rhodium atom of

the bridged species in the transition state (see Figure 3 middle). From the transition state, the maximum energy point on the reaction coordinate, the oxygen directly moves into the bridged position, energetically downhill. The activation energy is calculated to be 1.50 eV, considerably lower than the activation energy on the low-index (111) plane at an analogue surface coverage (2.2 eV, $\theta = 0.125^{[6]}$). The electron donation from the rhodium surface to the NO on the stepped surface (Mulliken charges: N: -0.23 e; O: -0.26 e) is not much different from that on the low-index (111) surface (Mulliken charges: N: -0.24 e, O: -0.22 e). This suggests that a higher activity of the stepped surface is more likely due to steric than to electronic effects.

To verify this assumption, the geometries of the reactant, the transition state and the product structure of the NO dissociation reaction were compared. The distances which the oxygen atom has to cover in the different steps of the dissociation process are given in Table 3. On Rh(311) the O atom of

Table 3. Distance of the oxygen atoms in the product [O(p)], the transition state [O(ts)] and the reactant structure [O(r)] of the NO dissociation on a stepped Rh(311) and a plane Rh(111) surface.

Distances [Å]	Rh(111)	Rh(311)
O(r)–O(ts)	2.26	1.29
O(ts)–O(p)	1.21	1.53
O(r)–O(p)	3.36	2.71

intact NO [O(r)] is much closer to its transition-state position than on Rh(111). Additionally, the distance which the oxygen atom has to cover to reach its position in the product structure is by far smaller on the stepped rhodium surface.

NO Dissociation in the Presence of Oxygen Preoccupation

An additional oxygen in a threefold hollow on the (111) terrace, adjacent to the NO molecule (see Figure 4), exhibits a direct influence on the electron transfer. The partial charges on the nitrogen and on the oxygen atom were determined by Mulliken population analysis to be -0.21 and -0.23 e, respectively. On the corresponding low-index (111) surface the elec-

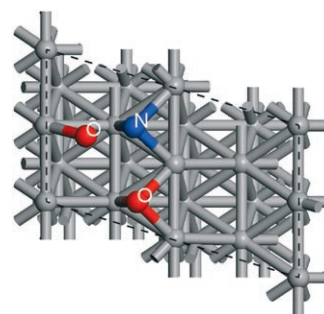


Figure 4. Transition state of the nitrogen monoxide dissociation on Rh(311) in the presence of an oxygen atom.

tron donation to the NO molecule is only slightly different (N: -0.23 e; O: -0.21 e). The net electron transfer of the surface to the NO molecule is equivalent on both planes (0.44 e) according to Mulliken population analysis.

Calculating the potential energy surface for the dissociation reaction allows the determination of its activation energy, which is 1.71 eV. The reaction is still exothermic in the presence of oxygen, but the energy gain is smaller (-0.19 eV).

While Mulliken charges of NO on stepped and plane surfaces are only slightly different, the activation energy (2.26 eV) is considerably higher than on the stepped surface (1.71 eV). The thermochemistry is inverted when changing the surface from stepped to plane (stepped: $\Delta E_{\text{react}} = -0.19$ eV, plane: $\Delta E_{\text{react}} = 0.14$ eV).

To investigate the influence of the preoccupation in more detail, the PES for the NO dissociation was calculated for a range of oxygen preoccupations ($\theta_{0,\text{init}} = 0.25, 0.5$ and 0.75) in analogy to a previous study.^[5] Comparing the activation energies for the NO dissociation on (111) and (311) surfaces as a function of the initial coverage (θ_{init}) shows that the activation barrier is lower on the stepped surface at any initial coverage (Figure 5). Nevertheless, the activation barrier increases with increasing initial coverage for the stepped as well as the plane surface.

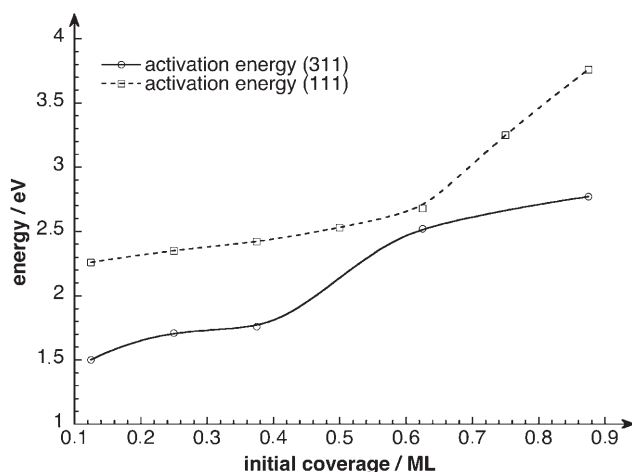


Figure 5. Comparison of activation energies for the NO dissociation on stepped Rh(311) and plane Rh(111) surfaces with different initial coverages.

To determine if the origin of this effect is electronic or steric or a combination of both, the electron transfer from the surface to the adsorbate was compared to the evolution of the activation energy. As can be seen from Figure 6, the reduction in the electron transfer and the increase of the activation barrier with increasing initial coverage correlate. This indicates that electronic effects indeed affect the activation barrier of the dissociation reaction. The electronegative oxygen withdraws electrons from the metal surface and hence lowers the back-donating effect of the metal to the antibonding π -orbital of the adsorbed NO species. The more oxygen coadsorbates are pres-

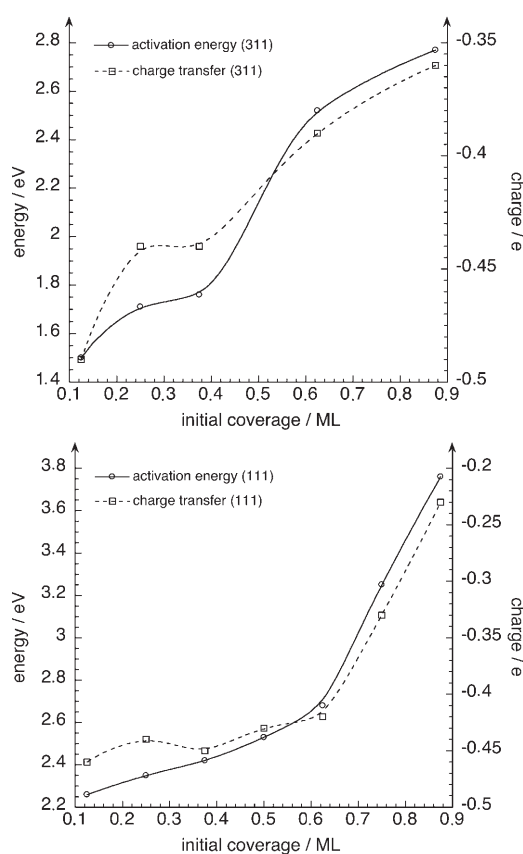


Figure 6. Comparison of net electron transfer and activation barrier of the dissociation reaction on the (311) and the (111) facets of rhodium (taken from ref. [6]).

ent, the lower is the electron donation to the NO molecule and the higher is the activation barrier for the NO dissociation.

However, as already mentioned, the net electron transfer of Rh(311) to NO at an initial coverage of 0.125 ML does not differ from the net electron transfer on Rh(111), while the activation barrier is 46.7% higher on the plane surface. Comparing the net electron transfer of Rh(311) and Rh(111) to NO as a function of the initial coverage shows no large differences in the activation energies (Figure 7). This indicates that not only electronic but also steric effects play a major role here.

Occupancy of the d-Band

As the charges calculated by Mulliken population analysis are not accurate, our interpretations were verified by calculating the d-band occupancy of the decomposing rhodium atom, which binds the oxygen in the transition state (Figure 8, Rh^4).

Firstly, the d-state-projected density of states (d-PDOS) of the decomposing rhodium atom on the clean Rh(311) was calculated. Secondly, the d-PDOS of this atom was calculated in the presence of NO ($\theta_{\text{NO}} = 0.125$) and with various oxygen precoverages ($\theta_{\text{O}} = 0.25, 0.5, 0.75, \theta_{\text{NO}} = 0.125$). The change of the d-PDOS (Δ d-PDOS) of the decomposing rhodium atom, induced by coadsorbates, was calculated by subtracting the d-

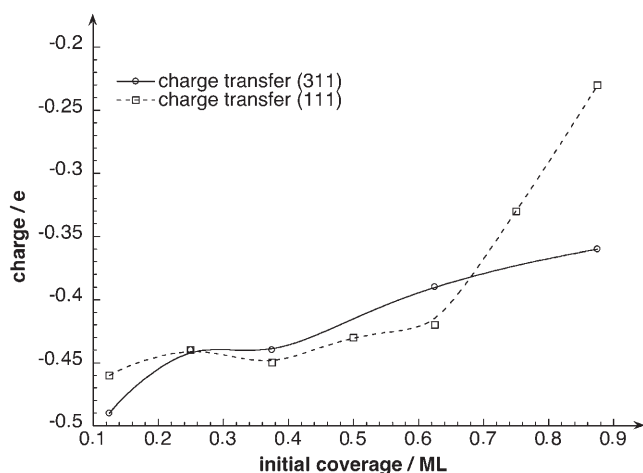


Figure 7. Net electron transfer of the (311) and the (111) facet of rhodium to NO as a function of the initial coverage.

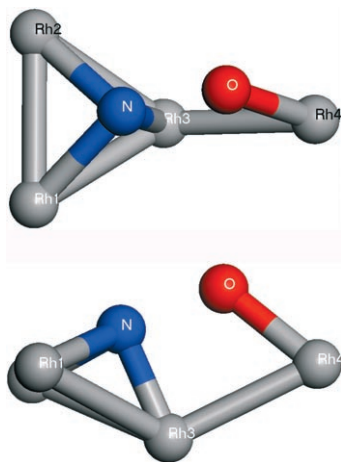


Figure 8. Atom numbering used in Table 6.

PDOS of the clean surface from the adsorption system according to Equation (4).

The d-band population difference, Δn_d , in Table 4 shows that with increasing coverage the d-states of the decomposing rhodium atom lose electron density. This is in agreement with our charge analysis of the transition-state structure: the higher the coverage is, the less occupied are the d-states and consequently, the lower is the electron donation to the transition-state structure.

Coverage (ML)	Δn_d [e]	ΔE_d [eV]
0.125	-0.006	-0.22
0.625	-0.189	-5.17
0.875	-0.211	-6.16

Hence, the stabilisation of the transition state decreases with increasing oxygen precoverage and consequently, the activation barrier of the reaction increases.

This effect is particularly profound when adsorbates are directly bound to the decomposing rhodium atom ($\theta = 0.625, 0.875$). In the transition state the oxygen of the decomposing NO competes with the adsorbate of the preoccupation, which both try to bond with the metal d-states around E_F . To illustrate this effect the Δd -PDOS of the decomposing rhodium atom of NO/Rh(311) with and without oxygen coadsorbates are illustrated in Figure 9. It can be seen that the Δd -PDOS be-

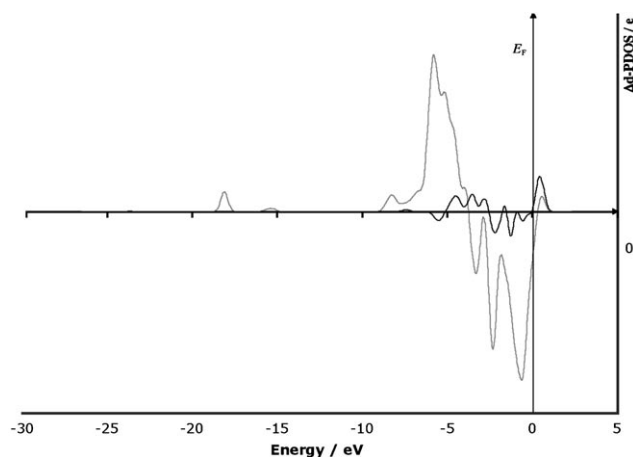


Figure 9. Δd -PDOS of the step-edge rhodium atom of Rh(311) covered with NO (black line) and NO with 0.75 ML oxygen (grey line).

neath the Fermi energy ($\varepsilon = -5$ to 0 eV) is slightly negative in case of NO as adsorbate (Figure 9, black line), while it is strongly negative with 0.75 ML oxygen coverage (Figure 9, grey line). Therefore, the electron density offered to the oxygen in the transition state is lower.

This leads to a competition between the oxygen precoverage and the transition-state oxygen atom for electron density beneath E_F . This competition for electron density induces a surface-mediated repulsion which weakens the stabilisation of the transition state, the so-called bonding competition effect.^[28] The bonding competition effect depends on the strength of the bonds to the metal atom. As both adsorbates are oxygen atoms and oxygen binds strongly to rhodium, this effect is exceptionally distinct herein.

Thermochemically the NO dissociation becomes less probable with increasing initial coverage as well (see Figure 10). In the case of Rh(111) the reaction is endothermic at any oxygen preoccupation. The endothermicity increases with increasing initial coverage.

In the case of Rh(311) the reaction is exothermic at low coverages, while it becomes thermoneutral at approximately 0.4 ML initial coverage according to our extrapolation. Above 0.4 ML the reaction is endothermic and its endothermicity increases with increasing initial coverage. However, thermochemically, the dissociation is more likely on the stepped surface than on the plane surface at any initial surface coverage.

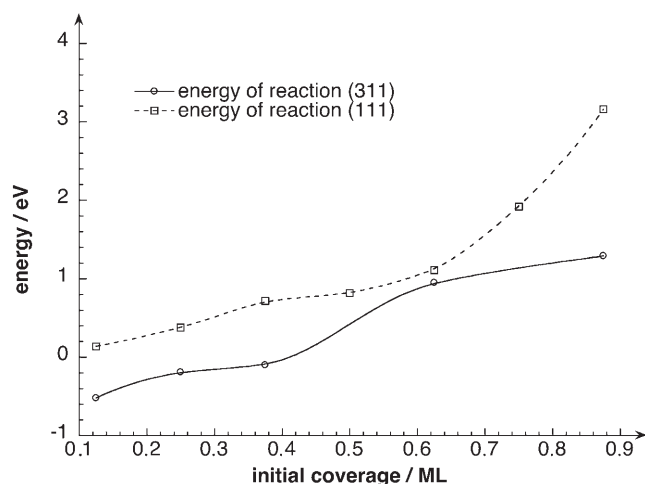


Figure 10. Reaction energy of the NO dissociation on Rh(311) and Rh(111) surfaces as a function of the initial coverage.

NO Dissociation in the Presence of Further Coadsorbates

The influence of further molecules, present in the real catalytic converter, on the NO dissociation on stepped surfaces has also to be considered.

Replacing oxygen as coadsorbate on the (111) terrace of the Rh(311) surface (see Figure 4) by molecules, such as SO and CO, and recalculating the PES for the NO dissociation leads to the following kinetic and thermochemical parameters (Table 5).

Table 5. Activation energy and reaction energy for the NO dissociation on Rh(311) with different coadsorbates.		
Coadsorbate	E_{act} [eV]	ΔE_{react} [eV]
without	1.50	-0.52
SO	1.39	-0.4
CO	1.60	-0.2
O	1.71	-0.19

Since all coadsorbates are electron-withdrawing one would expect that the activation energies are all higher than the activation energy for the dissociation of the solely adsorbed NO. Therefore, it is striking to see that in the case of SO as a coadsorbate the activation energy decreases in contrast to all other coadsorbates. Even though the electron transfer of NO coadsorbed with SO, compared to solely adsorbed NO, decreases the activation energy decreases.

Comparing the transition-state positions of the oxygen atom in the NO dissociation with and without SO as coadsorbate (Figure 11) shows that the transition-state position of the oxygen atom is shifted when SO is present. The displacement is most likely due to electrostatic repulsion of the partially negative-charged oxygen atoms of SO and NO. Figure 11 shows that oxygen in the transition state of the coadsorbed scenario is shifted towards the decomposing metal atom. Furthermore, the distance to its position in the reactant structure decreases. The decrease in the activation barrier is thus—in analogy to

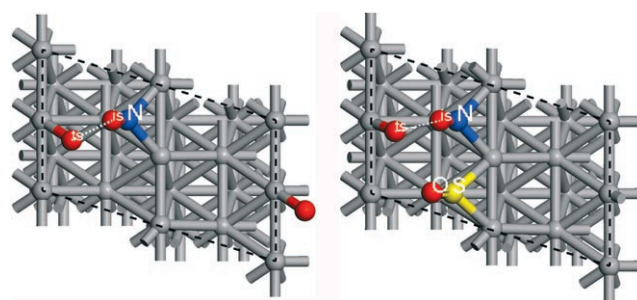


Figure 11. Comparison of the oxygen position in the initial state [O(is)] and the transition state [O(ts)] during the NO dissociation in the absence of a coadsorbate (left) and in the presence of SO (right).

the observed difference between plane and stepped surfaces—due to steric rather than electronic effects.

This result supports the earlier findings that electronic effects do influence the reaction, but are exceeded by steric effects.

Relationship between Activation and Reaction Energy

Plotting the activation energy as a function of the calculated reaction energy reveals an almost linear relationship (Figure 12). This phenomenon is referred to as Brønsted–

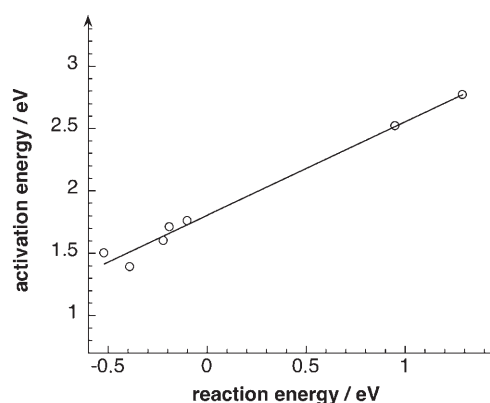


Figure 12. Activation energy as a function of the reaction energy of the studied NO dissociation.

Evans–Polanyi (BEP) relationship. A possible explanation for this linear relationship is the electron-withdrawing effect caused by coadsorbates. The higher the precoverage with those adsorbates is, the lower is the electron donation from the surface to the transition state of the surface reaction. The lower the electron donation is, the weaker is the bonding of the transition state to the surface and consequently the weaker is its stabilisation. Hence, the activation barrier of the decomposition increases. In analogy, the lower the electron transfer to the reaction products is, the weaker is the bonding of these atomic adsorbates and consequently the lower is the energy gain (the higher is the energy loss) of the reaction. Charge analysis as well as density of states analysis support this assumption.

Table 6. Transition-state geometries, for atom numbering see Figure 8.

Coadsorbates	<i>d</i> [Å]			O–Rh4	N–O	ϵ [°]	γ [°]
	N–Rh1	N–Rh2	N–Rh3				
without	2.20	1.97	1.90	2.00	1.80	114.9	89.9
O	2.14	2.20	1.92	1.98	1.83	114.8	89.3
2xO	2.23	1.97	1.90	2.04	1.73	113.9	93.1
4xO	2.23	2.03	1.91	2.03	1.86	108.2	87.4
6xO	2.30	2.08	1.90	2.05	1.84	104.5	92.1
CO	2.07	1.98	2.01	1.91	1.83	116.5	87.5
SO	2.13	2.05	1.90	1.99	1.80	114.4	91.4

The findings for Rh(311) are in agreement with observations on Rh(111).^[5,29] However, in case of Rh(111) the competitive bonding effect can be excluded as source of this relationship, since at none of the investigated precovered coadsorbates bind to the decomposing rhodium atom.

Conclusions

We showed that steric effects exceed electronic effects on the dissociation of NO on rhodium with and without coadsorbates. The electron donation of NO adsorbed on the (111) facet is almost equal to that on the (311) facet. However, the activation energy of the dissociation is considerably lower on the (311) than on the (111) facet. This is most likely due to the fact that the O atom of the NO is rather close to its position in the transition state and to the product structure on the stepped surface. Nevertheless, when considering the same surface geometry, electronic effects influence the activation barrier of the reaction.

These assumptions are supported by the findings for the NO dissociation with SO as coadsorbate. Electrostatic repulsion directs the oxygen atom of NO towards its transition-state position and even though the electron transfer decreases, the activation barrier decreases. This supports the hypothesis that both steric and electronic effects affect the activation barrier, but the steric effects exceed the electronic. Furthermore, this study supports earlier findings that coverage-dependent kinetic parameters have to be taken into account for microkinetic modelling of surface reactions.

Furthermore, the presented data support the catalytic mechanism proposed by Nakatsuji.^[30] If NO preferably decomposes at steps of a rhodium surface, a high concentration of atomic nitrogen builds up at those step sites. Inside this nitrogen-rich microenvironment nitrogen could recombine around step sites without diffusing over longer distances. This is a possible explanation of the surface chemistry of NO_x-dissociation catalysts. However, to verify this assumption the behaviour of oxygen at these step sites should be studied as well.

Acknowledgments

We gratefully acknowledge the financial support of the German Research Foundation (DFG) via the collaborative research center

“Reactive Flows, Diffusion, and Transport.” (SFB 359). O. R. I. is thankful to M.Sc. Monica Tutuianu for fruitful discussions.

Keywords: density functional calculations · heterogeneous catalysis · nitrogen oxides · rhodium · surface chemistry

- [1] D. A. King, *Science* **2004**, *303*, 176–177.
- [2] F. Garin, *Appl. Catal. A* **2003**, *222*, 183–219; L. S. Glebov, A. G. Zakirova, V. F. Tret'yakov, T. N. Burdeinaya, G. S. Akopova, *Petr. Chem.* **2002**, *42*, 143–172; F. Garin, *Catal. Today* **2004**, *89*, 255–268.
- [3] S. Kureti, W. Weisweiler, K. Hizbullah, *Appl. Catal. B* **2003**, *43*, 281–291.
- [4] T. Nakatsuji, V. Komppa, *Catal. Today* **2002**, *75*, 407–412; T. Nakatsuji, V. Komppa, *Appl. Catal. B* **2001**, *30*, 209–223.
- [5] O. R. Inderwildi, D. Lebiez, O. Deutschmann, J. Warnatz, *J. Chem. Phys.* **2005**, *122*, 154702.
- [6] O. R. Inderwildi, D. Lebiez, O. Deutschmann, J. Warnatz, *J. Chem. Phys.* **2005**, *122*, 034710.
- [7] L. A. DeLouise, N. Winograd, *Surf. Sci. Lett.* **1985**, *159*, A462.
- [8] S. H. Payne, H. J. Kreuzer, W. Frie, L. Hammer, K. Heinz, *Surf. Sci.* **1999**, *421*, 279–295.
- [9] N. M. H. Janssen, A. R. Cholach, M. Ikai, K. Tanaka, B. E. Nieuwenhuys, *Surf. Sci.* **1999**, *382*, 201–213.
- [10] E. H. Backus, A. Eichler, M. L. Grecea, A. W. Kleyn, *J. Chem. Phys.* **2004**, *121*, 7946.
- [11] B. Hammer, *Surf. Sci.* **2000**, *459*, 323; Z.-P. Liu, P. Hu, *J. Am. Chem. Soc.* **2003**, *125*, 1958–1967.
- [12] E. Balázs, G. Varga, L. Füstöss, *Surf. Sci.* **2001**, *482–485*, 1145–1151.
- [13] R. Apel, D. Fariás, H. Tröger, E. Kirsten, K. H. Rieder, *Surf. Sci.* **1996**, *364*, 303–311.
- [14] F. Esch, A. Baraldi, C. Comelli, S. Lizzit, M. Kiskinova, P. D. Cobden, B. E. Nieuwenhuys, *J. Chem. Phys.* **1999**, *110*, 4013–4020.
- [15] Y. Y. Sun, H. Xu, Y. P. Feng, A. C. H. Huan, A. T. S. Wee, *Surf. Sci.* **2004**, *548*, 309–316.
- [16] S. Liepold, N. Elbel, M. Michl, W. Nichtl-Pecher, K. Heinz, K. Müller, *Surf. Sci.* **1990**, *240*, 81–84.
- [17] T. C. Bromfield, D. C. Ferré, J. W. Niemantsverdriet, *ChemPhysChem* **2005**, *6*, 254.
- [18] D. K. Zerkle, M. D. Allendorf, M. Wolf, O. Deutschmann, *J. Catal.* **2000**, *196*, 18–39; O. Deutschmann, L. D. Schmidt, *AIChE J.* **1998**, *44*, 2465–2476.
- [19] M. D. Segall, P. L. D. Lindan, M. J. Probert, C. J. Pickard, P. J. Hasnip, S. J. Clark, M. C. Payne, *J. Phys. Chem. B* **2002**, *106*, 2717–2743.
- [20] J. P. Perdew, J. A. Chevary, S. H. Vosko, K. A. Jackson, M. R. Pederson, C. Fiolhais, *Phys. Rev. B* **1992**, *46*, 6671–6678.
- [21] D. Vanderbilt, *Phys. Rev. B* **1990**, *41*, 7892–7895.
- [22] H. J. Monkhorst, J. D. Pack, *Phys. Rev. B* **1976**, *13*, 5188–5192.
- [23] N. Govind, M. Petersen, G. Fitzgerald, D. King-Smith, J. Andzelm, *Comput. Mater. Sci.* **2003**, *28*, 250–258.
- [24] M. D. Segall, R. Shah, C. J. Pickard, M. C. Payne, *Phys. Rev. B* **1996**, *54*, 16317.
- [25] L. Köhler, G. Kresse, *Phys. Rev. B* **2004**, *70*, 165405; G. Kresse, A. Gil, P. Sautet, *Phys. Rev. B* **2003**, *68*, 073401.
- [26] B. Hammer, *Phys. Rev. Lett.* **1999**, *83*, 3682.

- [27] O. R. Inderwildi, A. Sundermann, **2003**, personal communication.
[28] Z.-P. Liu, *Pure Appl. Chem.* **2004**, *76*, 2069–2083; J. J. Mortensen, B. Hammer, J. K. Nørskov, *Surf. Sci.* **1998**, *414*, 315.
[29] O. R. Inderwildi, D. Lebedez, J. Warnatz, *Phys. Chem. Chem. Phys.* **2005**, *7*, 2552.

- [30] T. Nakatsuji, *Appl. Catal. B* **1999**, *21*, 121.

Received: April 20, 2005

Revised: August 16, 2005

Published online on November 18, 2005